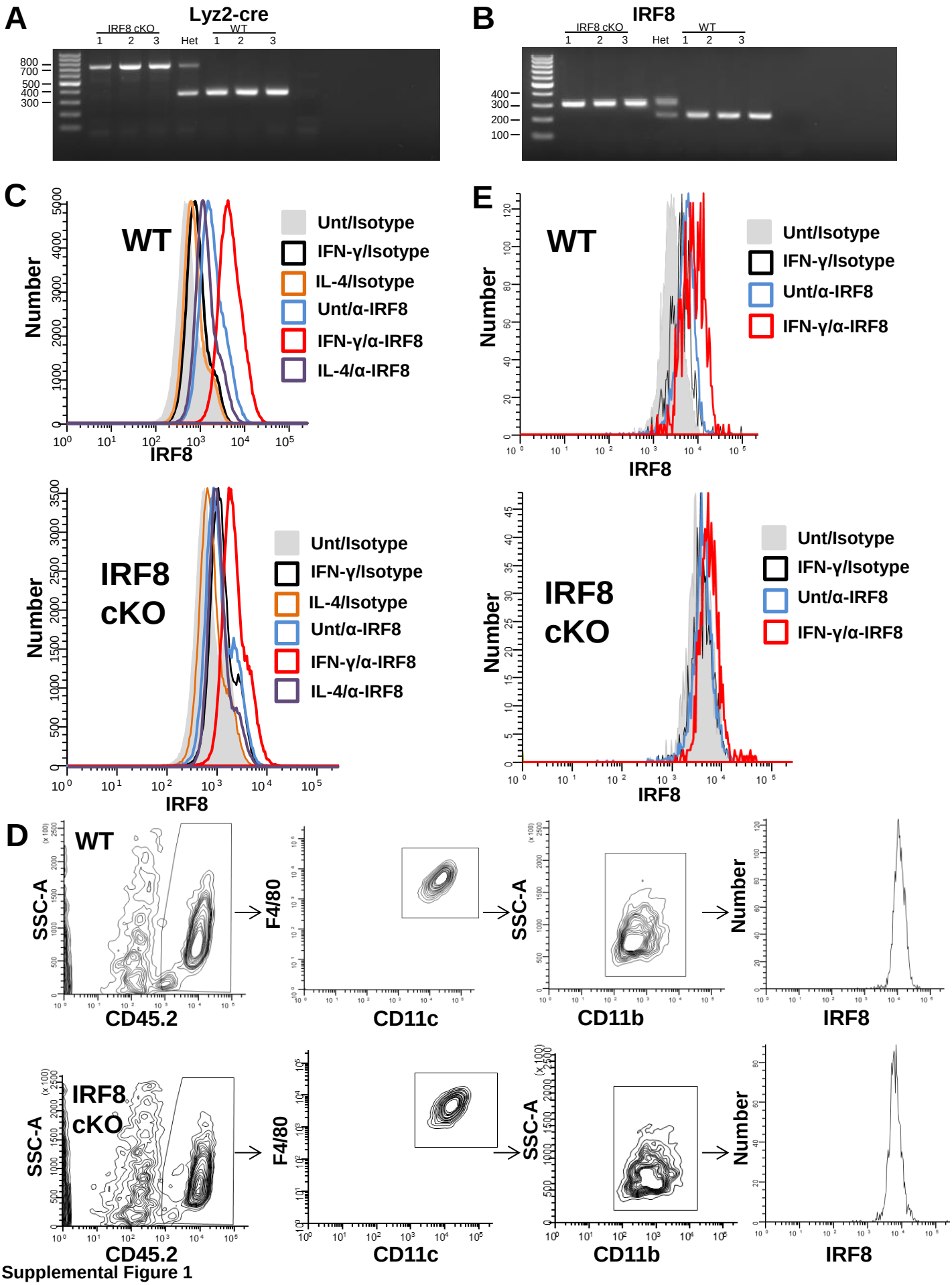

Supplemental Figure 1

Supplemental Figure 1. **Genotyping of WT and IRF8 cKO mice.** Tail DNA from WT ($IRF8^{fl/fl}$) or IRF8 cKO mice (n=3 each) was isolated and used for PCR to detect (***A)*** *Lyz2-Cre* and (***B***) the deleted IRF8 band. Heterozygous mice have features of both WT and IRF8 cKO genotypes. (***C)*** Flow cytometry histogram of intracellular IRF8 staining in BMDMs from WT or IRF8 cKO mice after treatment with vehicle (untreated), IFN-γ (100 U/ml) or IL-4 (20 ng/mL) for 24 hours. (***D***) Gating strategy for BAL-derived macrophages from WT or IRF8 cKO mice following treatment with IFN-γ (100 U/ml for 24 hours). (***E)*** Flow cytometry histogram of intracellular IRF8 staining in BAL-derived macrophages from WT or IRF8 cKO mice after treatment with vehicle (untreated) or IFN-γ (100 U/ml) for 24 hours.

A

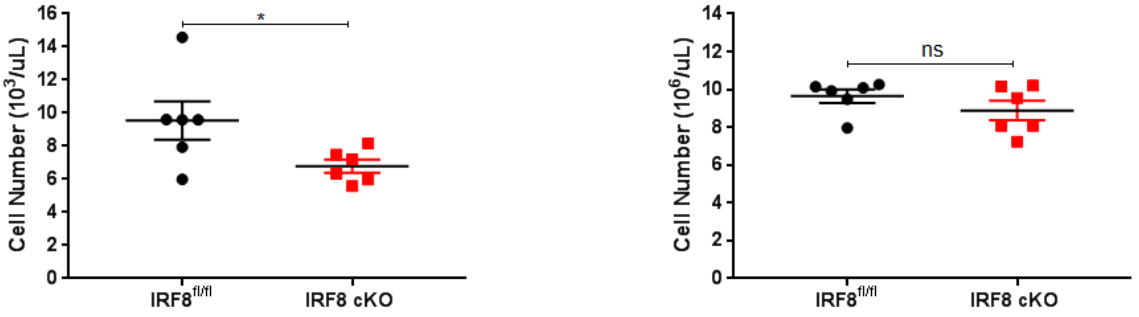

B

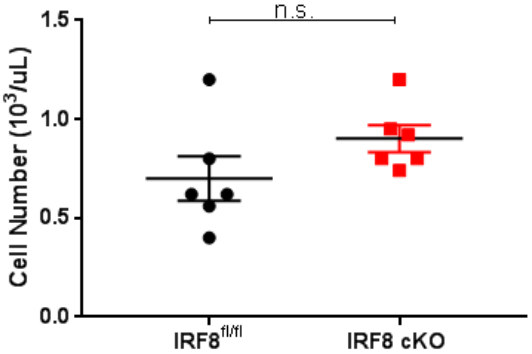

C

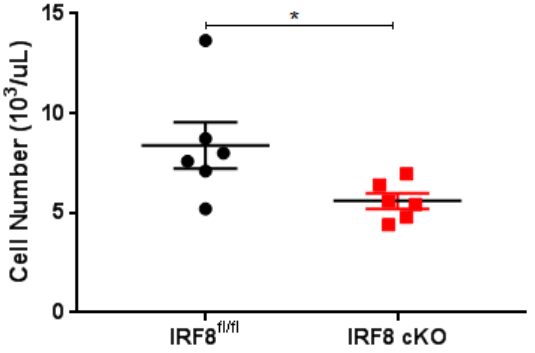

D

	IRF8 $^{fl/fl}$ (control)		IRF8 cKO	
	% of spleen	Absolute number (x10^7)	% of spleen	Absolute number (x10^7)
Macrophages	10 ± 1	0.8 ± 0.3	13 ± 3	1.3 ± 0.4
B cells	59 ± 3	4 ± 1	56 ± 3	5.0 ± 1
CD3$^+$ T cells	22 ± 1	1.0 ± 0.3	22 ± 3	2.0 ± 0.3
Granulocytes	10 ±1	1 ± 0.2	11 ± 1	1.0 ± 0.3

***Supplemental Figure 2*. Analyses of immune cell populations in WT and IRF8 cKO mice.**

Retro-orbital blood draws were performed in WT (IRF8$^{fl/fl}$) or IRF8 cKO mice, and the type, absolute number, or percentage of the indicated blood cells were quantified by an automated CBC instrument. (***A***) WBC (*left panel)* or RBC (*right panel*) counts, (***B***) granulocytes, (***C***) total lymphocytes, or ***(D)*** macrophages, B cells, CD3$^+$ T cells or granulocytes. Data recorded as mean ± SEM and significance determined by a 2-tailed Mann-Whitney test. In all panels, WT (n=6) or IRF8 cKO (n=6). *P<0.05; n.s., not significant

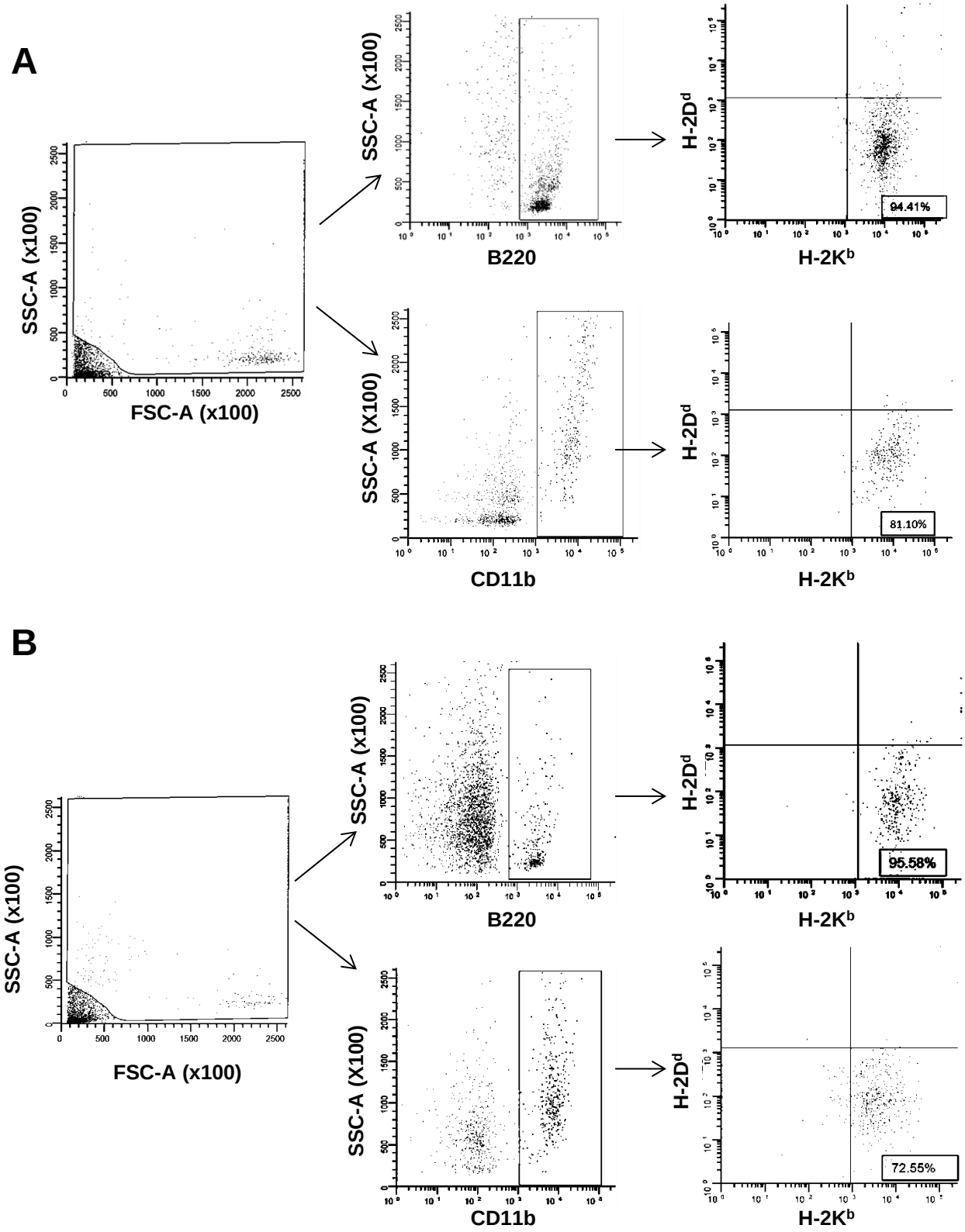

Supplemental Figure 3*. Reconstitution proficiency of donor WT or IRF8 cKO bone marrow cells following transplant.** Representative flow cytometry plots of B cells or total ($CD11b^+$) myeloid populations in the peripheral blood of (A***) WT or (***B***) IRF8 cKO BM recipients 8 weeks post-transplant.

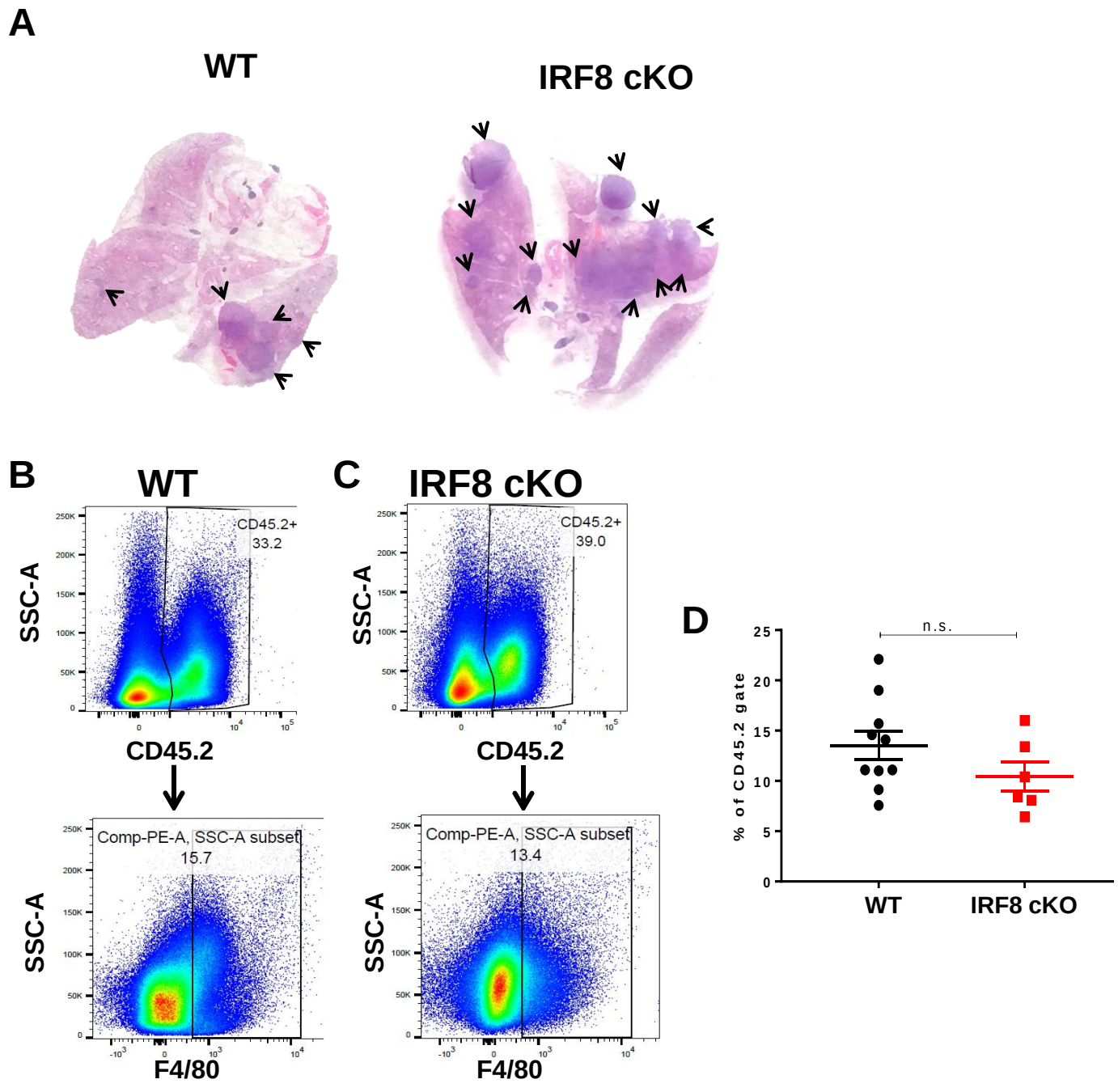

Supplemental Figure 4. **IRF8-deficiency in macrophages does not affect macrophage infiltration into primary tumors, but increases lung metastasis.** ***(A)*** H&E-stained whole lung from 4T1 tumor-bearing WT or IRF8 cKO mice. Metastatic nodules are indicated by arrows *(see Figure 2)* Representative flow plots of $CD45.2^{+}F4/80^{+}$ macrophages infiltrated within tumors of ***(B)*** WT or ***(C)*** IRF8 cKO recipient mice. ***(D)*** Quantification of macrophage infiltration into 4T1 tumors. Data recorded as mean ± SEM and significance determined by the 2-tailed Mann-Whitney test. n.s., not significant.

A

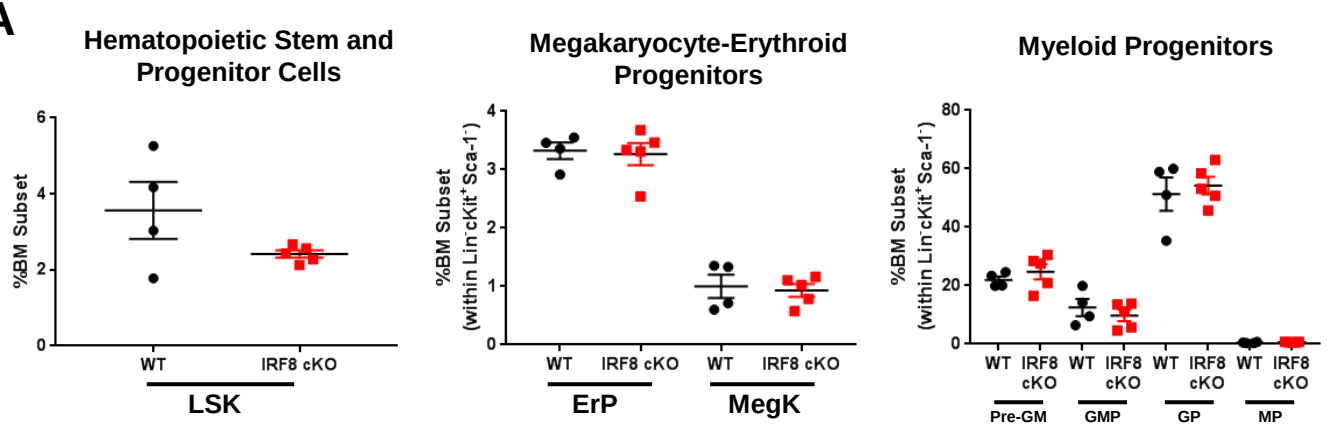

B

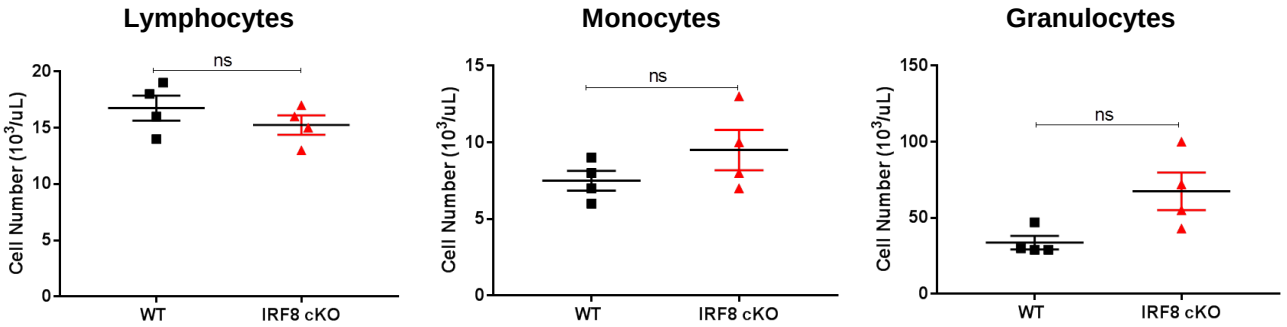

C

	WT			IRF8 cKO		
Cell Type	**Spleen**	**Tumor**	**Lung**	**Spleen**	**Tumor**	**Lung**
F4/80⁺ Macrophages	12 ± 2	29 ± 17	23 ± 6	16 ± 6	38 ± 14	34 ± 8
Gr-1⁺ Granulocytes	45 ± 7*	22 ± 12	72 ± 6	62 ± 6*	38 ± 18	82 ± 7
CD11c⁺ Dendritic cells	3 ± 0.4	16 ± 4	4 ± 1	3 ± 2	16 ± 6	4 ± 1
CD4⁺ T cells	5 ± 1	5 ± 3	3 ± 1	5 ± 2	5 ± 7	4 ± 2
CD8⁺ T cells	3 ± 1	4 ± 2	4 ± 2	3 ± 1	4 ± 2	4 ± 1

Supplemental Figure 5*. Characterization of bone marrow progenitor or peripheral immune cell populations in WT or IRF8 cKO tumor-bearing recipients.** Evaluation of major progenitor or peripheral immune populations from 4T1 tumor-bearing recipients that had received bone marrow from WT or IRF8 cKO mice. (A***) Percentages of the indicated bone marrow progenitors, as performed in Figure 1, in tumor-bearing WT or IRF8 cKO recipients at endpoint, as in Figure 2. (***B***) Absolute numbers of lymphocytes (*left*), monocytes (*middle*) or granulocytes (*right*) were quantified by an automated CBC instrument. (***C***) Percentages of major immune cell populations in the spleen, primary tumor or lung of WT or IRF8 cKO recipients, as determined by flow cytometry. Cells were gated on the CD45.2⁺ population, as in Supplemental Figure 4. Data recorded as mean ± SEM and significance determined by a 2-tailed Mann-Whitney test. Each data point represents a single mouse in ***A*** & ***B***. In ***C***, WT (n=4) or IRF8 cKO (n=5). **P*<0.05; ns, not significant

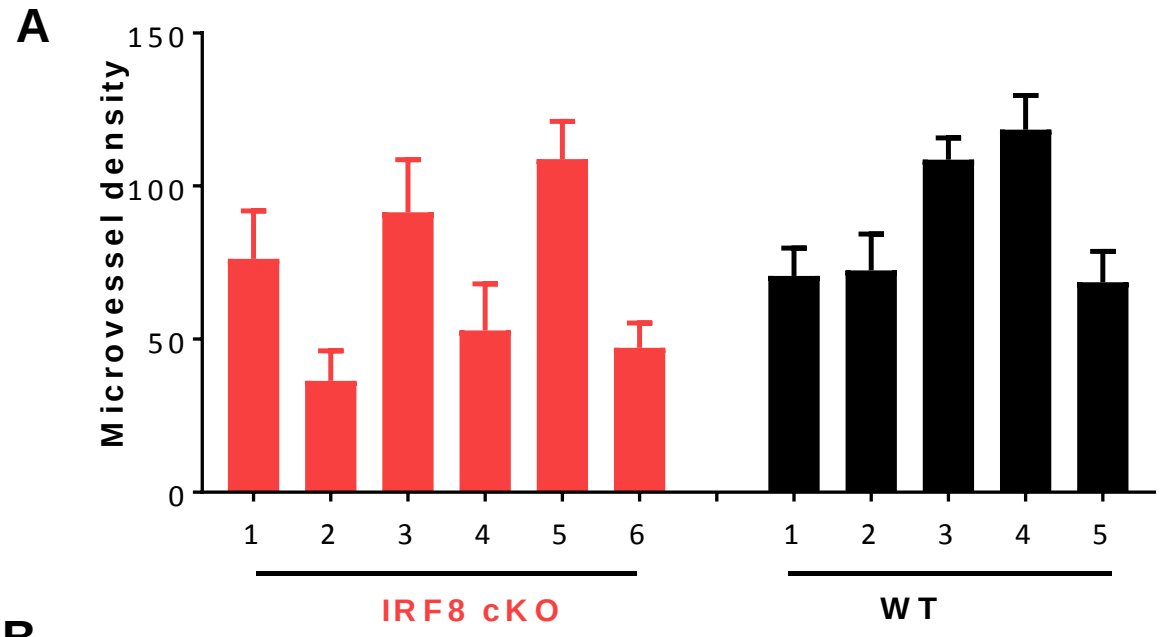

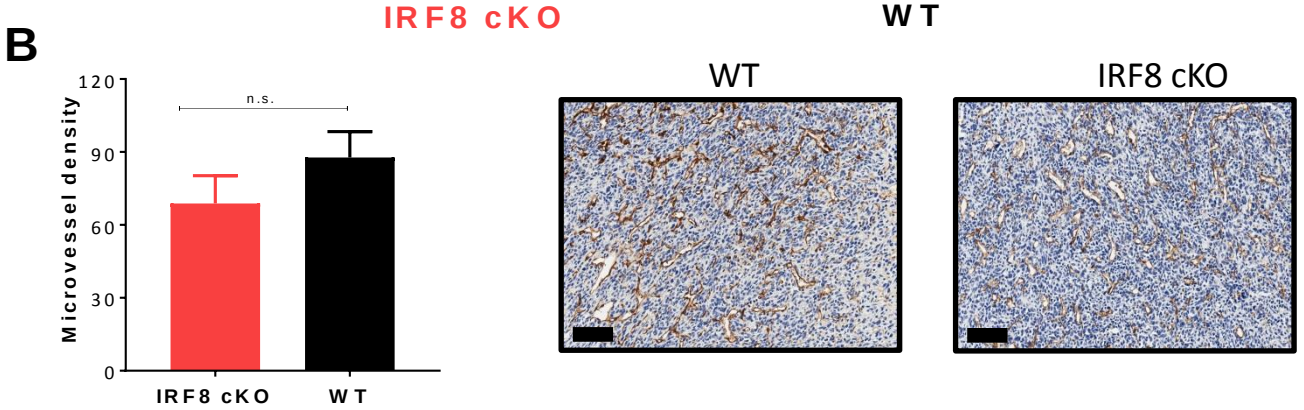

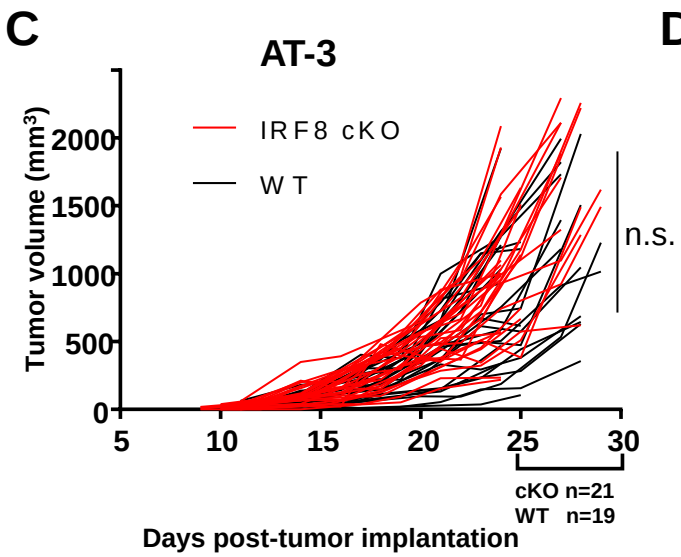

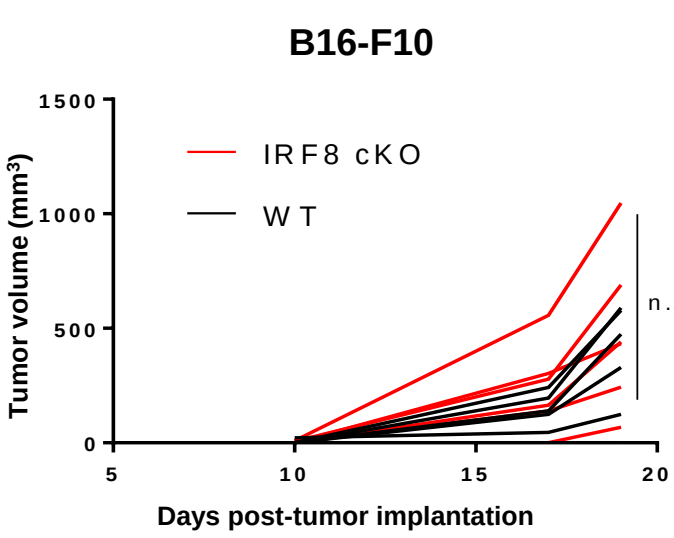

Supplemental Figure 6

Supplemental Figure 6*. Reduced IRF8 expression in macrophages does not affect microvessel density or increase tumor growth in primary tumors.** WT or IRF8 cKO BM recipients were implanted with 4T1 cells, as in Figure 1. The entire tumor tissue was removed ~30 days later, and stained with anti-CD31 antibody to identify endothelial cells for quantification of microvessel density. (A***) Individual microvessel density counts of each mouse. X-axis represents mouse ID numbers. (***B***) Average microvessel density in the WT or IRF8 cKO groups. Representative IHC images of anti-CD31 staining. Data were not significantly (n.s.) different by the 2-tailed Mann-Whitney test (mean ± SEM of 5 mice per group) (***C***) Tumor growth of WT (n=25) or IRF8 cKO (n=31) mice implanted orthotopically with AT-3 mammary tumor cells ($1x10^5$). Tumor growth was not significantly different (mean ± SEM of 25 to 31 mice per group). Data are compiled from 4 separate experiments. (***D***) Tumor growth of B6 WT (n=5) or IRF8 cKO (n=6) mice implanted with B16-F10 tumor cells SQ in the left flank ($1x10^5$). Tumor growth was not statistically significant different.

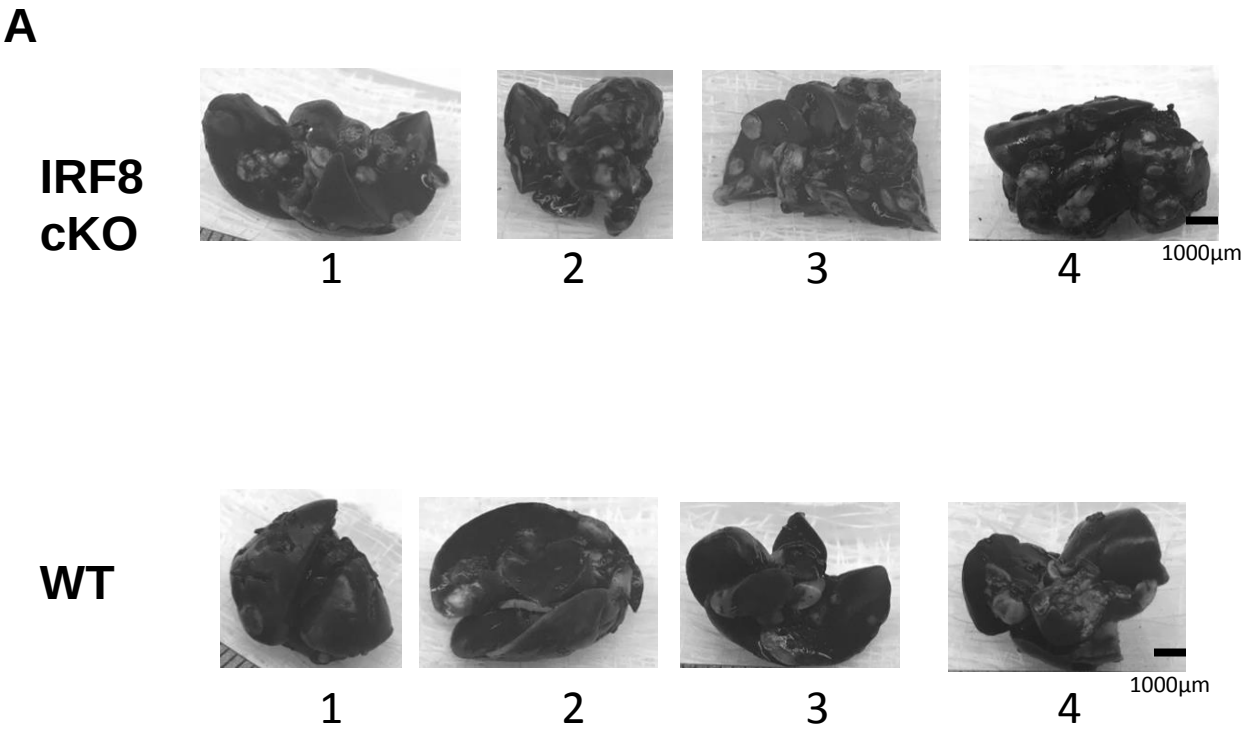

Supplemental Figure 7. **Reduced IRF8 expression in macrophages increases experimental lung metastasis.** 4T1 cells ($5x10^4$) were injected intravenously into chimera mice reconstituted with WT ($IRF8^{fl/fl}$) or IRF8 cKO bone marrow cells, as in Figures 2 and 4. Lung tumor burden was determined ~30 days later. Lung weights post-India ink staining in non-tumor bearing WT ($IRF8^{fl/fl}$) or non-tumor-bearing IRF8 cKO mice (n=4 each) or the corresponding tumor-bearing groups are shown in Figure 4. Here, photographs of whole mouse lung after India ink staining revealed white metastatic nodules against a black tissue background.

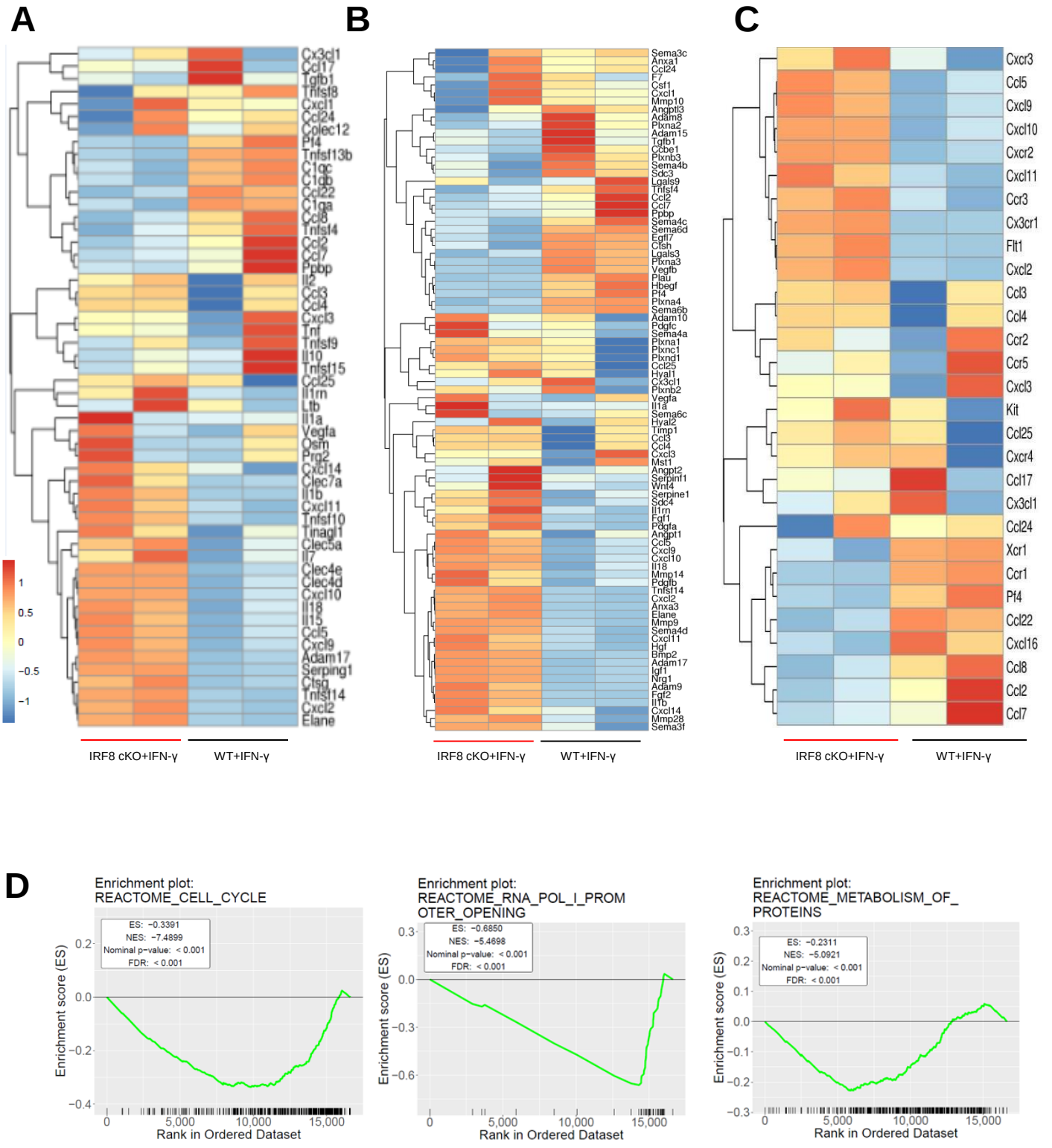

Supplemental Figure 8*. Reduced IRF8 expression in macrophages alters transcriptome of genes tied to immunity, cell migration and neutrophil chemotaxis.** (A-C***) Transcriptome analysis of BMDMs from WT or IRF8 cKO mice (n=2 biologic replicates each) after treatment with IFN-γ (100 U/mL) for 24 hours. Heat-map depicting gene sets involved in (***A***) immune response, (***B***) cell migration, and (***C***) neutrophil chemotaxis. *(See Figure 5)* (***D***) GSEA for examples of pathways downregulated in IRF8 cKO model.

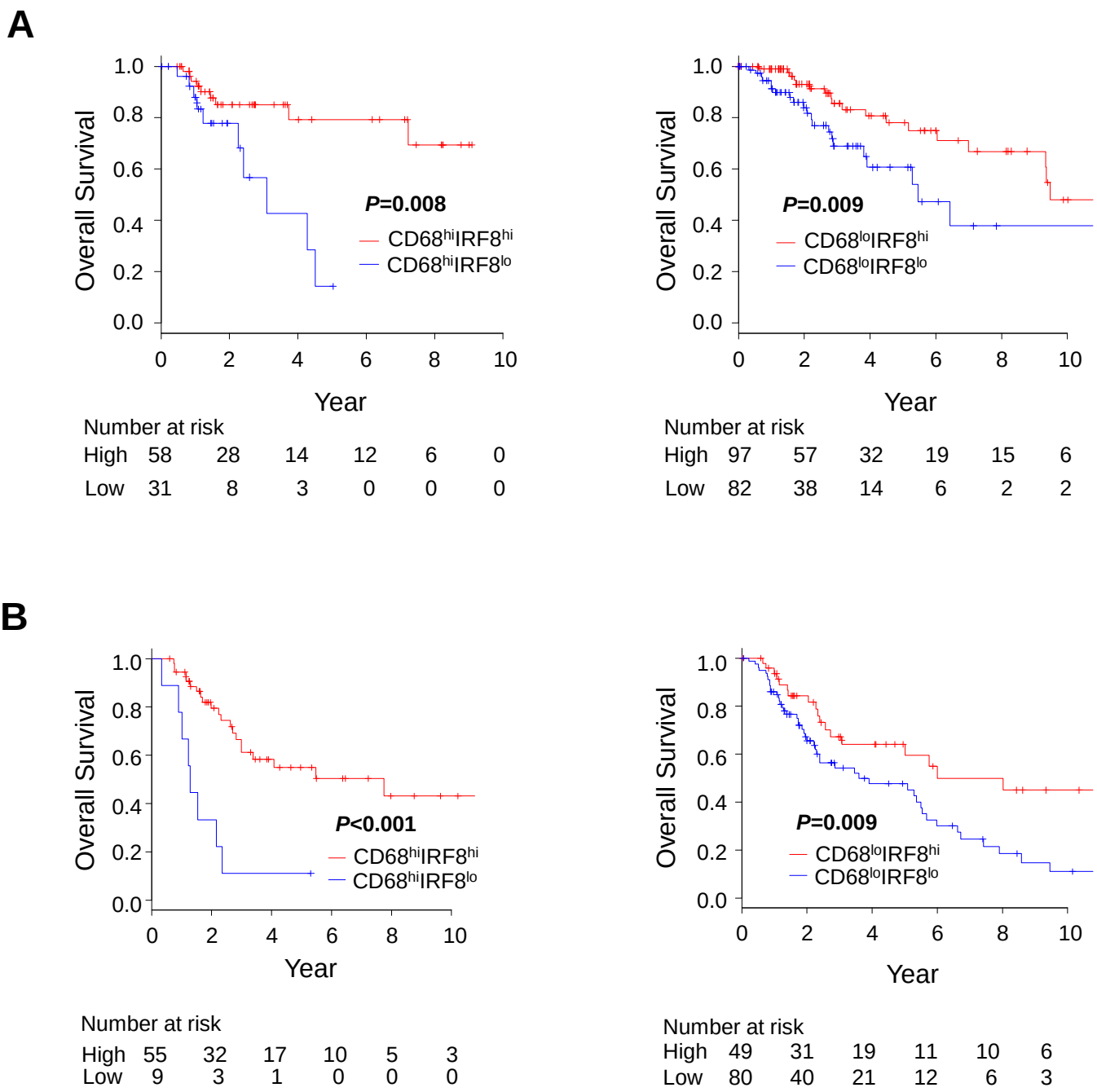

Supplemental Figure 9. **A macrophage signature with higher IRF8 expression compared to lower IRF8 expression is associated with increased survival in late-stage breast cancer and melanoma patients.** (***A***) Kaplan-Meier survival curves based on TCGA data from Figure 6 showing a profile of higher IRF8 expression compared to lower IRF8 expression in stage III/IV breast cancer patient tumors within a $CD68^{+}$ macrophage cohort [high (n=89 patients; *left panel*) or low (n=179 patients; *right panel*) macrophage infiltration] correlates with improved overall survival. IRF8 stratification is shown under 'number at risk'. (***B***) Kaplan-Meier survival curves in stage III/IV melanoma patients based on TCGA data from Figure 6 and illustrated as in ***A*** [high (n=64 patients; *left panel*) or low (n=129 patients; *right panel*) macrophage infiltration]. Statistical analysis of the survival curves was determined by the log-rank test.

Antigen/marker	Clone	Catalog number	Company
CD16/32	2.4G2	560540	BD Biosciences
Ly6A/E (Sca-1)	E13-161.7	122513	BioLegend
Ly6G/Ly6C(Gr-1)	RB6-8C5	108409	BioLegend
CD135 (Flt3)	A2F10	135305	BioLegend
CD117 (c-Kit)	30-F11	47-0451-82	eBioscience
Ly6C	RB6-8C5	108421	BioLegend
CD11b	M1/70	563553	BD Biosciences
CD11c	N418	117335	BioLegend
CD8a	53-6.7	100708	BioLegend
CD150	TC15-12F12.2	115927	BioLegend
CD105	MJ7/18	48-1051-82	eBioscience
DAPI	N/A	D1306	ThermoFisher Scientific
H-2K^{b}	AF6-88.5	562002	BD Biosciences
H-2D^{d}	34-2-12	553579	BD Biosciences
B220	RA3-6B2	103247	BioLegend
F4/80	BM8	123110	BioLegend
CD45.2	104	552950	BD Biosciences
IRF8	REA516	130-108-196	Miltenyi Biotec
CD31	MEC 13.3	550274	BD Biosciences
Goat anti-rat Ig	N/A	554014	BD Biosciences
Fixable Viability Stain	N/A	565388	BD Biosciences

Supplemental Table 1: **Antibodies used for flow cytometric analyses.**

Mouse Primer Name	Sequence
Lyz2-Cre mutant	CCC AGA AAT GCC AGA TTA CG
Lyz2-Cre common	CTT GGG CTG CCA GAA TTT CTC
Lyz2-Cre wildtype	TTA CAG TCG GCC AGG CTG AC
IRF8$^{fl/fl}$ Fwd	TTG GGG ATT TCC AGG CTG TTC TA
IRF8$^{fl/fl}$ Rev	CAC AGG GAG TCC CTC TTA CAA T
GAPDH Fwd	CAT CAC CAT CTT CCA GGA GCG
GAPDH Rev	GCT GAA TGG TGT GTG TCA TAG GC
iNOS Fwd	ACA AGC TGC ATG TGA CAT CG
iNOS Rev	GGC AAA GAT GAG CTC ATC CA
Arg1 Fwd	GTG AAG AAC CCA CGG TCT GT
Arg1 Rev	CTG GTT GTC AGG GGA GTG TT
β-actin Fwd	CTG GCA CCA CAC CTT CTA CAA TG
β-actin Rev	GGG TCA TCT TTT CAC GGT TGG
Ccl5 Fwd	ATG GCT CGG ACA ACC ACT CCCT
Ccl5 Rev	GGT TGG CAC ACA CTT GGCG
Cxcl2 Fwd	GAA GTC ATA GCC ACT CTC AAGG
Cxcl2 Rev	TTC CGT TGA GGG ACA GCA
Elane Fwd	TGT GAA CGT ATG CAC TCT GG
Elane Rev	CGA AGG CAT CTG GGT ACA AT
MMP9 Fwd	ACG ACA TAG ACG GCA TCC AGT ATC
MMP9 Rev	AGG TAT AGT GGG ACA CAT AGT GGG
S100A8 Fwd	TGC CAC ACC CAC TTT TAT CA
S100A8 Rev	GAG TGT CCT CAG TTT GTG CAG
S100A9 Fwd	AGA TGG CCA ACA AAG CAC CT
S100A9 Rev	TAA AGG TTG CCA ACT GTG CT

Supplemental Table 2: **Sequences for RT-PCR and quantitative RT-PCR primers**